J Solid State Electrochem (1999) 3: 179–186

ORIGINAL PAPER

B.J. Eastwood · P.A. Christensen
R.D. Armstrong · N.R. Bates

Electrochemical oxidation of a carbon black loaded polymer electrode in aqueous electrolytes

Received: 23 July 1998 / Accepted: 17 November 1998

Abstract The suitability of a polymeric composite material for use as part of an anode structure in a cathodic protection system has been examined. The composite material was a conductive blend (volume resistivity typically 1.5 Ω cm) of carbon black in a polyethylene binder. A long operational lifetime for the material demands that the rate of carbon loss must be low. In the work reported here, electrochemical and *in situ* analytical techniques were employed to characterise the performance of the material over a wide range of anodic current densities in a variety of aqueous electrolytes. The predominant anodic electrochemical reaction on the polymeric material is CO_2 formation in acid and neutral solutions, which causes loss of carbon from the surface and the development of a non-conducting layer of polyethylene. The characteristics of the reaction suggest that it occurs via the discharge of H_2O. In alkaline pH, however, the anodic reactions are more complex. A high OH^- concentration (pH 12 or higher) favours the formation of oxygen rather than CO_2, particularly at low anodic potentials. The presence of CO_3^{2-} in the electrolyte catalyses the evolution of oxygen at pH values as low as 9. The electrochemical formation of oxygen always occurs in parallel with the generation of some humic acid in the solution.

Key words Cathodic protection system · Carbon oxidation · Composite carbon/polymer anode · Lifetime

Introduction

Compared with the body of literature which exists on the gas phase oxidation of carbon, there is little available information on the electrochemical oxidation of carbon in aqueous solution [1]. Recent interest in the electrochemical dissolution of carbon has been sparked by its increasing use as an electrode support material in batteries and fuel cells [2–6]. Ross et al. [7–10] have studied carbon blacks and catalysed blacks for their resistance to anodic dissolution in alkaline solutions. They found that the more graphitic the black the more resistant it was to oxidation to CO_2. The nature of carbon black surfaces has been recently reviewed by Fabish and Schleifer [11] and Boehm [12].

Krishtalik et al. [13–19] and Kokhanov et al. [20–22] have studied the electro-oxidation of graphite electrodes in aqueous electrolyte. They found that the predominant electrochemical reaction for graphite in contact with sulfate and phosphate electrolytes, for acid to neutral pH, was the formation of CO_2, and that oxygen evolution only occurred with high efficiency at pH values greater than 11. These authors also found that there was significant conditioning of the carbon electrodes in the sense that the currents at a fixed potential increased with time. In addition to the electrochemical formation of O_2 and CO_2, other reactions which have been reported to occur when carbon/graphite is used as an anode are the incorporation of ions in the graphite structure [23] and the formation of "humic acid" in the solution [24].

The aim of the work reported in this paper was to elucidate the mechanisms of the steady state electrochemical reactions at a carbon black/polyethylene composite material (in aqueous solution) which could be used as part of an anode structure in a cathodic protection system. The carbon black used was Ensaco MS (MMM, Belgium). Ensaco MS is a medium-structure carbon black with a macro structure of acetylene black that has surface characteristics of furnace blacks. It was chosen because of its purity, low Brunauer Emmett Teller (BET) surface area and high native pH, all of which favour stability towards (electrochemical) oxidation. These properties may be attributed to its highly graphitic character.

B.J. Eastwood · P.A. Christensen · R.D. Armstrong (✉)
Chemistry Department, University of Newcastle,
Newcastle upon Tyne, NE1 7RU, UK

N.R. Bates
Raychem Ltd, Swindon SN3 5HH, UK

Experimental

Electrode materials

The polymer composite electrode material used throughout this investigation was a blend of Ensaco MS carbon black (41 w/w) in linear low-density polyethylene. The material has a typical volume resistivity of 1.5 Ω cm [25]. The specification for Ensaco MS carbon black is given in Table 1. Two differently shaped electrode types were fabricated out of the conductive polymer material. The first, type 1, were cylindrical electrodes formed by extruding the polymer through a 13 mm die around a central copper core (which acted as the current collector). The polymer electrode material shields the copper core from any contact with the electrolyte. This system represents the form in which the material could be used in commercial systems. One end of these electrodes was blanked off using standard epoxy resin, and PTFE tape was wrapped around the opposite end to give electrodes of varying lengths. The second form of electrode, type 2, may be described as "top-hat" shaped. These electrodes were hot pressed between sheets of steel, giving a different surface finish to that of the type 1 electrodes. Type 2, "top-hat", electrodes were employed as the working electrodes for the *in situ* Fourier transform infrared (FTIR) spectro-electrochemical measurements described below. The counter electrodes, with the exception of the FTIR experiments, were high surface area 99.9% Pt gauze. A coil of 99.99% Pt wire (ca. 20 cm long, 1.0 mm diameter) was employed in the FTIR spectro-electrochemical cell.

Electrolytes

The electrolytes employed for the purpose of this study were aqueous solutions of H_2SO_4, Na_2SO_4, H_3PO_4, NaH_2PO_4, Na_2HPO_4, $NaHCO_3$, Na_2CO_3, $C_8H_5O_4K$ (potassium hydrogen phthalate) and NaOH or aqueous solutions of mixtures of the chemicals listed. All of the salts employed were analytical grade (BDH or Fluka) with the exception of the $NaHCO_3$, Na_2CO_3 and NaOH used for the bulk of the experiments, which were BDH general purpose reagents. To check that this had no effect on the results, key experiments were repeated using Fluka analytical grade salts. No change was found in the observed behaviour. In general the reagents were employed at 0.1 M concentration in 18 MΩ cm (Millipore) water. The 0.1 M Na_2SO_4 + 5 mM H_2SO_4 electrolyte (pH 2.5) will be referred to as the "standard sulfate" and 0.1 M Na_2CO_3 + 0.1 M $NaHCO_3$ (pH 10) as the "standard carbonate" electrolyte. H_2SO_4 and NaOH solutions were used to change the pH of solutions to the required values.

Electrochemical measurements

The cyclic voltammetry, potentiostatic and galvanostatic experiments were carried out using an Oxsys Micros Electrochemical Interface incorporating fast computer control via an Atari computer. The power output of this system was, however, limited to 20 mA at 10 V. Therefore for higher currents an EDT ECPI30 galvano-potentiostat was used. In both cases, potentials and currents were measured using Keithley 175 multimeters. All potentials are quoted with respect to a Ag/AgCl reference electrode (4 M KCl, E = 0.207 V vs. NHE [26]). Galvanostatic experiments were carried out using polymer anode (PA) electrodes of both types 1 and 2 detailed above, with and without stirring. Current densities were selected to give approximately evenly spaced data points on a logarithmic scale, and a time of 10 min was allowed at each current to allow the system to reach a steady state. During measurements the current density at which the PAs were held was decreased from the maximum to minimum value because of the significant "conditioning" (see below) of the anodes that occurs. Cyclic voltammograms were routinely collected before and after the experiments as an additional means of monitoring the electrochemical behaviour. The anodic potential limits were selected to encompass the anodic potentials observed in the steady state experiments, and the cathodic limit was chosen to coincide with the onset of hydrogen evolution.

Some steady state measurements were made using a rotating disk system consisting of a 5.4 mm diameter, hot pressed, PA disk electrode which had been machined to size from a top-hat electrode. The magnitude of disk currents during cyclic voltammetry experiments were also recorded for voltammograms captured at different disk rotation speeds. All measurements were made at room temperature (22 ± 3 °C).

Table 1 The specification of Ensaco MS carbon black

Property	Value
Specific surface area	45 ± 3 $m^2\ g^{-1}$ (BET)
DBP (dibutyl phthalate) value	350 cm^3 $(100\ g)^{-1}$
Particle diameter (average)	70 nm
pH value	7–8
Volatile matter	0.15%
Water content	0.25%
Ash content	0.05%
Grit (+325 mesh)	0.002–0.0002 wt%
Electrical resistivity	0.25 Ω cm (at 50 kg cm^{-2})

In situ oxygen detection

Oxygen produced in the electrochemical reaction was detected by a Clarke membrane-type oxygen electrode. The Clarke system (consisting of a base plate containing the Ag "horse-shoe" reference electrode and Pt disk working electrode, polarising circuitry and stirrer) was supplied by Rank Brothers Limited (Cambridge, UK). The electrochemical cell had a solution of 70 cm^3 and a gas phase volume 15 cm^3 in the working electrode compartment, which was interfaced with the Clarke electrode base plate. The working electrode compartment was separated from the counter electrode compartment by a salt bridge, so as to prevent any oxygen generated at the working electrode from being reduced at the counter electrode. The system was calibrated by assuming that the concentration of O_2 in the initial aerated electrolyte was 2.82×10^{-4} mol l^{-1} [27]. The system was purged with N_2 to remove the atmospheric O_2 before use, and tested using O_2 evolution at a Pt electrode, where it was reasonable to assume 100% current efficiency for oxygen evolution.

Infra-red measurements

The *in situ* FTIR spectro-electrochemical measurements were carried out using a Bio-Rad FTS-60 spectrometer. The electrochemical cell employed has been described in detail elsewhere [28]. The FTIR experiments were used to monitor continuously any CO_2 produced during polarisation. The technique also allowed changes in the IR absorption of the electrolytes employed to be monitored.

Prior to each experiment the electrochemistry of the PA/electrolyte system under study was checked by capturing one complete cyclic voltammogram with the "top-hat" electrode pulled back from the CaF_2 window. The cell solution was then exchanged for fresh electrolyte and the electrode pushed forward against the CaF_2 window to trap a thin layer of electrolyte. The Bio-Rad FTS-60 spectrometer was purged with nitrogen. When no change in the absorptions characteristic of water or CO_2 were observed over a time of 20 min, the experiments were commenced. Single beam spectra were typically collected at 8 cm^{-1} resolution with 100 scans co-added and averaged per scan-set requiring ca. 5 s per scan set at

a detector speed of 125 kHz. After collecting the single beam reference spectrum R_0, potentiostatic or galvanostatic control of the PA was initiated. Spectra are presented as plots of $\Delta R/R_0$ versus wavenumber, where R_0 is the single beam reference spectrum captured at time zero, before polarisation was started, and ΔR is the result of subtracting the reference spectrum captured at time zero (R_0) from the single beam spectrum captured at time t (R_t) after beginning the polarisation.

UV-visible spectroscopy

UV-visible spectroscopy was carried out on the electrolytes using a Shimadzu UV-160 A spectrophotometer so as to provide additional information on the products of the anodic reactions.

Results

Steady state polarisation experiments

In all of the neutral and acidic pH electrolytes, the PA material showed well-defined Tafel behaviour (Fig. 1). Linear plots were obtained over more than 2 decades and the acidic pH systems were found to exhibit almost identical Tafel slopes (approx. 204 mV decade^{-1}), whether obtained from CVs or constant current polarisation experiments. In neutral and slightly alkaline pH sulfate and phosphate electrolytes the Tafel slope increased to approx. 270 mV decade^{-1}. The only deviation from linearity was observed towards zero current, where a slight increase in the Tafel slope was seen.

The galvanostatic polarisation experiments on PAs in alkaline solutions exhibited a more complex behaviour (Fig. 2) than that observed for PA electrodes in neutral to acidic pH electrolyte. In the absence of carbonate/bicarbonate ions, increasing the pH of the solution gave rise to the development of E-log i curves with distinct low-current and high-current Tafel regions. The presence of carbonate and/or bicarbonate ion caused the anodic reaction(s) to occur at much lower anodic potentials than in solutions of the same pH where carbonate species were absent. The inclusion of a Tafel plot for the PA material in pH 2.2 phosphate electrolyte in Fig. 2 shows that the behaviour at the higher current densities studied is almost identical between pH 2.2 and pH 11 [plots (ix) and (i), respectively], provided that carbonate species are not present. At pH values higher than 12 (in the absence of carbonate species) the high current density Tafel sections are found at much lower anodic potentials than in the acid/neutral solutions. However, deviation towards steeper Tafel slopes at the lower current densities is accentuated by increasing the pH.

None of the polarisation measurements were found to be rotation speed dependent.

Cyclic voltammetry

The CVs of the PAs in pH 2–11 electrolytes in the absence of carbonate species exhibited a common behaviour. A "conditioning" phenomenon was apparent in that PAs passed significantly greater currents at the (same) anodic potential limit after galvanostatic operation (Fig. 3). There was also a greater capacitative charging current after galvanostatic polarisation.

For solutions with pH values greater than 11 (in the absence of carbonate species) an autocatalytic feature was found in the first sweep owing to the very rapid

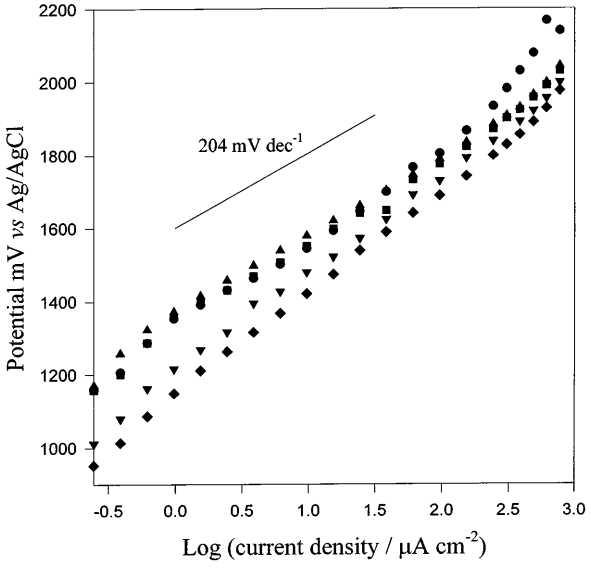

Fig. 1 Tafel plots for the galvanostatic polarisation of type 1 polymeric anodes (PAs) in various electrolytes: ● and ▲ pH 2.2, 0.1 M H_3PO_4; ■ pH 2.4, 0.1 M Na_2SO_4; ▼ pH 6, 0.1 M Na_2SO_4; ◆ pH 11, 0.1 M Na_2HPO_4

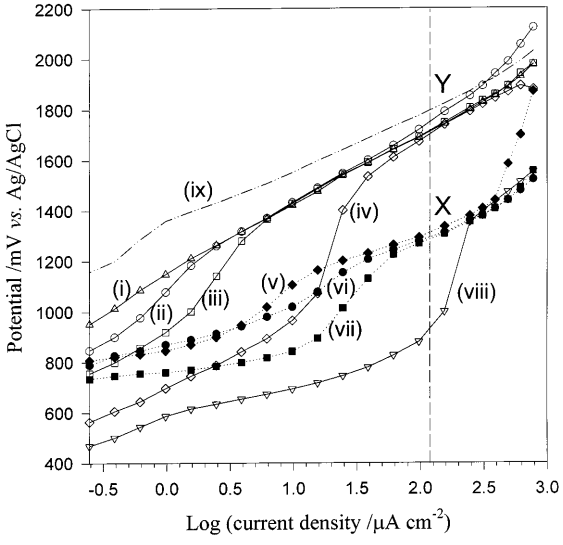

Fig. 2 Tafel plots for the galvanostatic polarisation of type 1 polymeric anodes in various electrolytes: (*i*) 0.1 M Na_2HPO_4, pH 11; (*ii*) 2 mM NaOH, pH 11.3; (*iii*) 10 mM NaOH, pH 11.8; (*iv*) 0.1 M Na_2SO_4, pH 12; (*v*) 0.1 M Na_2HPO_4 + 0.1 M Na_2CO_3, pH 11; (*vi*) 0.1 M Na_2CO_3 + 0.1 M HCO_3, pH 10; (*vii*) 0.1 M Na_2SO_4 + 0.1 M Na_2CO_3, pH 11; (*viii*) 0.1 M NaOH, pH 13.2; (*ix*) typical acid electrolyte curve

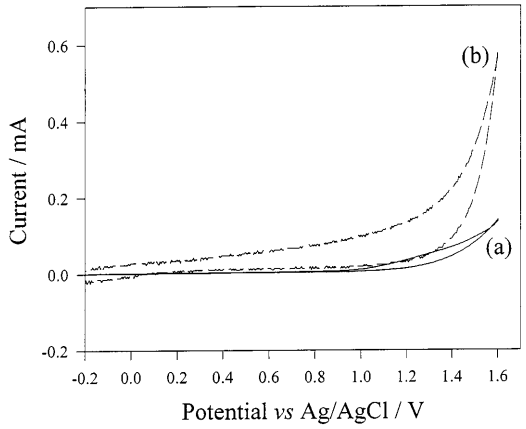

Fig. 3 Cyclic voltammograms (CVs) of a PA operated in 0.1 M Na_2HPO_4, pH 11 electrolyte: (*a*) initial CV of previously unused electrode; (*b*) "conditioned" electrode immediately after galvanostatic polarisation experiment. Electrode area 4.0 cm^2. Scan rate 100 mV s^{-1}

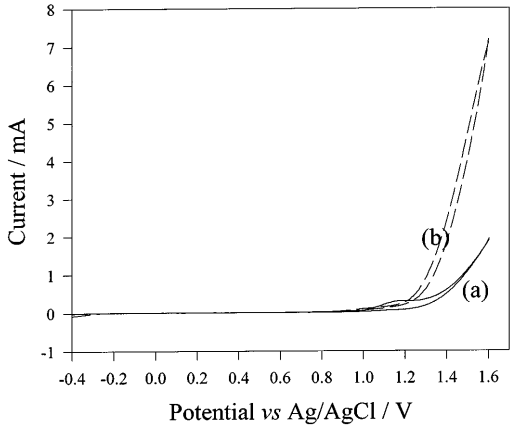

Fig. 5 CVs of a PA operated in aerated 0.1 M Na_2HPO_4 + 0.1 M Na_2CO_3, pH 11, electrolyte: (*a*) initial CV of previously unused electrode; (*b*) "conditioned" electrode immediately after galvanostatic polarisation experiment. Electrode area 4.0 cm^2. Scan rate 100 mV s^{-1}

activation of the electrode (Fig. 4) under these conditions. However, after galvanostatic operation there is little change in the current at a given potential. For solutions with carbonate species present, electrode conditioning was also apparent (Fig. 5), in the sense that at the anodic limit a much higher current density was apparent after galvanostatic operation.

Reaction product identification

The O_2 evolution efficiencies of the electrodes were measured at 125 μA cm^{-2} for each solution. This current density corresponds to the vertical dashed line shown in Fig. 2.

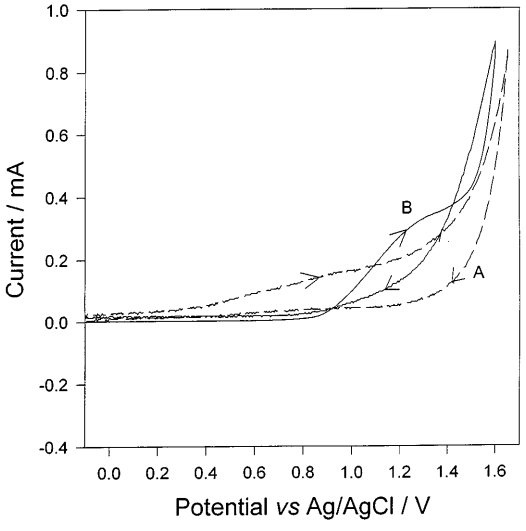

Fig. 4 CVs of a PA operated in 0.1 M Na_2SO_4, pH 12 electrolyte: *A* initial CV of previously unused electrode; *B* "conditioned" electrode immediately after galvanostatic polarisation experiment. Electrode area 4.0 cm^2. Scan rate 100 mV s^{-1}

For alkaline solutions, some typical results are shown in Table 2. In the absence of carbonate species there was a transition from low to high O_2 evolution efficiency as the pH of the solutions was increased to between 11 and 13. However, in the presence of carbonate species the efficiency for oxygen was 80% or greater if the pH was higher than 9. All log *i-E* plots in Fig. 2 which passed through X had O_2 efficiencies of at least 80%, whereas those which passed through Y had efficiencies of 10% or less. In long-term experiments where the solution pH was allowed to fall (as a result of the occurrence of the electrode reaction) the efficiency for oxygen fell with time. Some experiments were carried out at lower current densities. Measurements in the lower current density Tafel regions (approx. 10 μA cm^{-2}) showed a high current efficiency for oxygen evolution for solutions of NaOH (pH 13.2), SO_4^{2-} (pH 12) and SO_4^{2-}/CO_3^{2-} (pH 11). In the case of SO_4^{2-} (pH 12), this contrasts with the low oxygen current efficiency at higher potentials (125 μA cm^{-2}).

In acid and neutral solutions the current efficiency of the PA material for O_2 evolution was 5–10% at the start of galvanostatic polarisation. After 1 h the efficiency had fallen to less than 5%. After operation for a week the current efficiency was still less than 5%.

The FTIR measurements made using acid solutions are shown in Fig. 6. A gain feature can be seen near 2340 cm^{-1}, which can unambiguously be assigned to CO_2 [29]. The broad "rolling" bands that can be seen across the whole spectral region may be attributed to reflectivity changes in the electrode surface. The other significant feature was the development of a bipolar band centred near 1140 cm^{-1}, which may be assigned to changes in the "standard sulfate" electrolyte employed owing to the acidification of the thin layer electrolyte as a result of anodic polarisation. The negative lobe near 1190 cm^{-1} corresponds to hydrogen sulfate (HSO_4^-) gain, and the positive lobe near 1087 cm^{-1} corresponds to SO_4^{2-} loss [30]. There were also significant loss fea-

Table 2 The O_2 evolution efficiency of polymer anodes in alkaline solutions, measured at 125 μA cm^{-2}

Electrolyte	pH	O_2 evolution efficiency (%)	Comments
0.1 M $NaHCO_3$ + 0.1 M Na_2CO_3	10.4	>88	Efficiency improves with time
0.1 M Na_2HPO_4 + NaOH	11.0	<4	Efficiency deteriorates with time
0.1 M Na_2SO_4 + 0.1 M Na_2CO_3	11.1	>83	Efficiency improves with time
0.1 M Na_2HPO_4 + 0.1 M Na_2CO_3	11.1	>81	Efficiency improves with time
0.1 M Na_2SO_4 + NaOH	11.8	<11	Efficiency deteriorates with time
0.01 M NaOH	12.0	<28	Efficiency fallen to 7% in 25 min
0.14 M NaOH	13.2	> 83	Efficiency improves with time

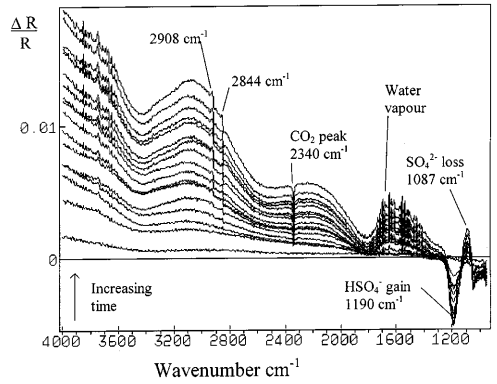

Fig. 6 *In-situ* Fourier transform infrared (FTIR) spectra of a "top hat" PA operated at 125 μA in N_2-sparged 0.1 M Na_2SO_4 + 5 mM H_2SO_4 (pH 2.5). Each spectrum was the result of 100 co-added and averaged scans at 8 cm^{-1} resolution. Time between each spectrum ca. 50 s

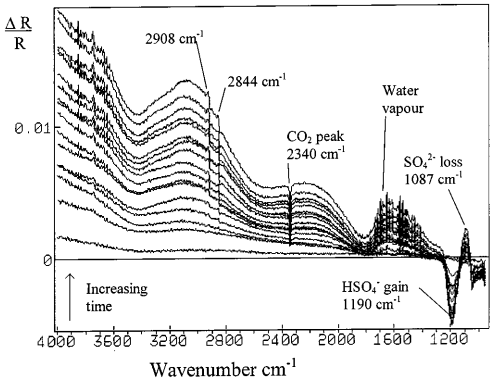

Fig. 7 *In situ* FTIR spectra of a "top-hat" PA operated at 125 μA in pH 10.4, 0.1 M Na_2CO_3 + 0.1 M $NaHCO_3$ electrolyte. Each spectrum was the result of 100 co-added and averaged scans at 8 cm^{-1} resolution. Time between each spectrum ca. 50 s

tures obvious at 2908 cm^{-1} and 2844 cm^{-1}, corresponding to the loss of C—H stretching frequencies.

Systems that were found to be highly O_2 evolution efficient initially showed very little evidence of CO_2 evolution in the FTIR experiments. There was an absence of the characteristic peak for CO_2 (at 2340 cm^{-1}) in the high pH electrolytes in which the Tafel plots passed through point X. This provides corroborative evidence that the PA/electrolyte systems with Tafel plots passing through point X do not result in the significant production of CO_2 from the anodic dissolution of the carbon electrode. However, after operation at high current densities and over prolonged operational times, some CO_2 production was observed. This can be attributed to the pH in the vicinity of the electrode falling (below 10) as a result of oxygen evolution. Another feature of the FTIR spectra collected during the galvanostatic control of the PA material at high current densities in carbonate containing electrolytes was the absence of any bipolar band attributable to CO_3^{2-} loss and HCO_3^- gain which might be expected due to the acidification of the electrolyte. A very strong peak at 1392 cm^{-1} was observed in the spectra (Fig. 7) corresponding to the loss of CO_3^{2-}. The expected peak for the gain of HCO_3^- did not appear. As in acid solutions, there were also significant loss features obvious at 2908 cm^{-1} and 2844 cm^{-1}, corresponding to the loss of C—H stretching frequencies.

All the systems which had high current efficiencies for oxygen evolution gave rise to a yellow/brown coloration in the electrolyte after polarisation at high current densities for 6–8 h. Continuous electrolysis caused the coloration to intensify over several days. At low current densities the formation of the coloured solution was not observed. Inductive coupled plasma (ICP) analysis showed that the yellow/brown coloration was not due to any metal ion contamination. The UV-visible spectrum showed a peak at ca. 240 nm with a long tail to longer wavelengths. It is consistent with the generation of mixture of humic acids in the solution [31] . Humic acids can be regarded as sections of the basal plane of graphite with a variety of oxygenated groups, particularly —COOH groups, attached. The UV-visible spectrum for the pH 2.5 "standard sulfate" electrolyte was measured after galvanostatic control of a PA for 5 days. Again a peak was found in the same region, though it is ca. 5% of that observed in the carbonate electrolyte after only 2 days of operation.

FTIR spectra of the coloured aqueous phase were taken after the solution volume was reduced and the solution had been neutralised. The resulting sample was extracted into dichloromethane and a spectra was run by evaporation of the organic phase onto a CaF_2 window. A typical spectrum of the organic extraction is shown in Fig. 8. The spectrum was dominated by peaks at 2848 cm^{-1} and 2918 cm^{-1} due to aliphatic C—H

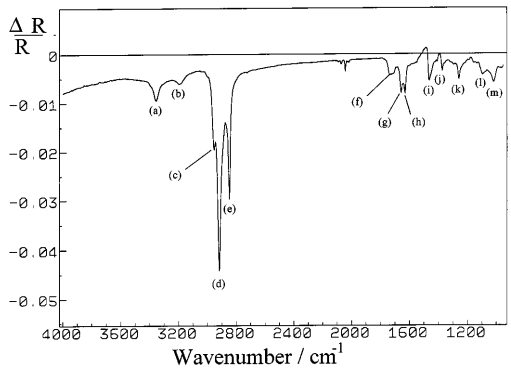

Fig. 8 Ex situ FTIR spectra of the organically extracted component of the electrolyte after long-term electrolysis. Electrolyte was pH 10, 0.1 M Na_2CO_3 + 0.1 M $NaHCO_3$. The difference spectrum shown is the result of 100 co-added and averaged scans at 8 cm^{-1} resolution with the blank CaF_2 disk providing the reference spectra. Peak assignments: (*a*) 3355 cm^{-1}, (*b*) 3193 cm^{-1}, (*c*) 2954 cm^{-1}, (*d*) 2918 cm^{-1}, (*e*) 2848 cm^{-1}, (*f*) 1730 cm^{-1}, (*g*) 1654 cm^{-1}, (*h*) 1630 cm^{-1}, (*i*) 1465 cm^{-1}, (*j*) 1373 cm^{-1}, (*k*) 1258 cm^{-1}, (*l*) 1095 cm^{-1}, (*m*) 1019 cm^{-1}

stretching bands [32], confirming the presence of organic species. Peaks corresponding to loss features at similar wavenumbers were also observed in the *in situ* experiments. Other peaks included one near 3435 cm^{-1}, believed to be due to O—H stretching, the peak at 1730 cm^{-1} due to C=O stretching, peaks at 1653 and 1610 cm^{-1} which could be due to quinone groups, and peaks in the range 370–1060 cm^{-1} due to various C—O stretching vibrations (carboxylic acids, lactones and esters) [33]. All of these species are characteristic of carbon black surface functionality, especially a surface that has been subjected to an oxidative treatment [11, 12], and are consistent with the presence of (a variety of) humic acids in the solution. The presence of the peaks at 2948 cm^{-1} and 2919 cm^{-1} corresponding to C—H stretching and at 1465 cm^{-1} and 1373 cm^{-1} corresponding to C—H_2 bending deformations could also indicate the presence of the polyethylene binder in the aqueous phase. The discrepancy between the large peak sizes at 2848 cm^{-1} and 2918 cm^{-1} and the much smaller peaks at 1465 cm^{-1} and 1373 cm^{-1} are more typical of carbon black FTIR spectra [6].

Changes in the electrical resistance of polymeric anodes after operation

The electrical resistance of the PAs were checked before and after galvanostatic measurements. A pointed metal probe attached to a digital resistance meter was pressed into the copper core at the centre of the PA, and the second probe was pressed firmly onto the WE surface of the PA. The electrical resistance of unused PAs measured in this fashion varied between 14 Ω and 16 Ω. After operation at 125 μA cm^{-2} in solutions which led to CO_2 formation as the dominant reaction, after a period of only 2 h, the electrical resistance of PAs was found to increase by an order of magnitude. At the end of the 4 day polarisation experiments, the surface of the PA had become highly resistive (with resistance greater >1 MΩ). The appearance of the PAs remained unchanged to the naked eye, even after 4 days of continuous operation. For solutions which were oxygen efficient, very little change was found in the resistance over a period of hours. After 4 days of continuous electrolysis the resistance had typically risen to ca. 500 Ω.

Discussion

For a carbon electrode in contact with an aqueous electrolyte it is a reasonable assumption that, in the absence of any other electro-active species, the long-term anodic process will be one, or both, of the electrochemical reactions (1) and (2) below:

$$2H_2O \rightarrow O_2 + 4H^+ + 4e^- \quad E^\circ = 1.229\ V \tag{1}$$

$$C + 2H_2O \rightarrow CO_2 + 4H^+ + 4e^- \quad E^\circ = 0.207\ V \tag{2}$$

Reaction (1) corresponds to oxidation of the aqueous electrolyte and (2) corresponds to anodic dissolution (or destruction) of the carbon anode. On thermodynamic grounds we would expect the formation of CO_2 to be the dominant reaction in acid, neutral and alkaline solutions. [In alkaline solution (pH 14) the reversible potentials for (1) and (2) are 0.404 V and −0.619 V, respectively]. Therefore only in situations where the kinetics of (1) are slow and that of (2) fast can oxygen evolution dominate. Our present results show that oxygen evolution is the dominant reaction only when the OH^- concentration is greater than 0.01 M or when CO_3^{2-} is present and the pH is at least 9.

In solutions of pH 2–9 (or 2–11 if no carbonate species were present), more than 90% of the anodic current passed was found to lead to the formation of CO_2. This is similar to previous reports for graphite [13–22] and carbon black [7–10]. The behaviour is independent of the pH and of the anion present and the Tafel slope is ca. 240 mV $decade^{-1}$. This suggests that the slow step in the reaction is the discharge of water onto the surface of the carbon black in a single electron transfer, which can be represented as

$$H_2O \rightarrow OH_{ads} + H^+ + e^- \tag{3}$$

Formation of CO_2 could follow as a result of the surface diffusion of two adsorbed OH species to the one carbon or the discharge of a second water molecule very near to the site of an OH_{ads}.

In strongly alkaline solutions, e.g. 0.1 M NaOH, the anodic reaction is predominantly oxygen evolution throughout the potential range explored. This reaction occurs at less anodic potentials than those found for CO_2 formation in neutral and acid solutions. Therefore

the oxygen evolution reaction must involve the discharge of OH^- to form OH_{ads} as

$$OH^- \rightarrow OH_{ads} + e^- \quad (4)$$

with the subsequent discharge of a further OH^- onto or very near OH_{ads} to form oxygen. This mechanism will explain the results if the rate of discharge of OH^- to form OH_{ads} is much more rapid than that of H_2O to form OH_{ads} at the same potential, and there is a high rate of discharge of OH^- onto (or very near) the site of OH_{ads}. The Tafel slope over most of the potential range is ca. 100 mV decade^{-1}, which suggests that the first OH^- discharge is rate determining. It is possible that the sites of OH^- discharge onto the carbon are different from those for H_2O discharge.

For alkaline solutions with no carbonate species present, and with pH values higher than 11 (such as the pH 12 solution of SO_4^{2-}) but less than 13, which give lines through point Y in Fig. 2, there is CO_2 formation at high current densities and oxygen evolution at low current densities, with a clear crossover between the two regions (see the schema in Fig. 9). The mechanism of CO_2 formation must be the same as that in acid solutions since the Tafel lines are the same at high anodic potentials. The shape of the Tafel plots at less anodic potentials can be explained if we assume the mechanism of oxygen evolution is reaction (4) followed by

$$OH^- + OH_{ads} \rightarrow O_2 + 2H^+ + e^- \quad (5)$$

where (5) is relatively potential independent. At low anodic potentials the rate determining step will be (4) whilst as higher anodic potentials it will be (5).

The measurements made here showed little dependence on either the anion or electrolyte concentration employed, except for the case of carbonate species. The presence of CO_3^{2-} anions gave rise to marked and systematic differences in Tafel plots, CVs and the anodic reaction products of otherwise identical electrolytes in the pH range 10–13. Most significantly it was found that the presence of CO_3^{2-} anions catalysed the O_2 evolution reaction, to the extent that the O_2 evolution reaction was the predominant reaction at all current densities in experiments carried out at pH > 10. This catalytic behaviour in the presence of CO_3^{2-} was accompanied by the formation of humic acids. The large loss feature found in the FTIR in Fig. 7 at 1396 cm^{-1} corresponds to CO_3^{2-} loss and the fact that there is no corresponding peak for HCO_3^- gain shows that CO_3^{2-} is playing an active part in the O_2 evolution mechanism. CO_3^{2-} is a highly oxidised species and further oxidation is not anticipated at the potentials employed. Therefore, the loss of the CO_3^{2-} must be due to intercalation of CO_3^{2-} into graphitic planes at the surface of the carbon black contained in the PA. In addition, the formation of an adsorbed planar surface CO_3^{2-} species is likely. The formation of planar CO_3^{2-} is possible on the significant areas of basal plane nature present in the Ensaco MS carbon black. If such species were adsorbed flat on the surface, they would be invisible to the IR beam owing to the operation of the surface selection rule [33, 34]. Since CO_3^{2-} catalyses the oxygen evolution reaction it is reasonable to assume that it is adsorbed on the carbon surface. The catalytic action of CO_3^{2-} in respect of oxygen evolution may be due to catalysis of OH^- discharge. The formation of highly active peroxycarbonate intermediates by the reaction

$$CO_{3ads}^{2-} + OH_{ads} \rightarrow C(O^-)OOH_{ads} + e^- \quad (6)$$

with subsequent decomposition of the peroxycarbonate is also possible. Peroxy-carbonate species are short lived, and once formed quickly dissociate to give O_2 [35]. When oxygen evolution has occurred for a significant length of time the carbon surface starts to disintegrate, giving rise to humic acids in the electrolyte. This disintegration is probably due to the carbon surface becoming highly oxidised under the conditions of oxygen evolution and the weakening of the graphite structure due to carbonate intercalation.

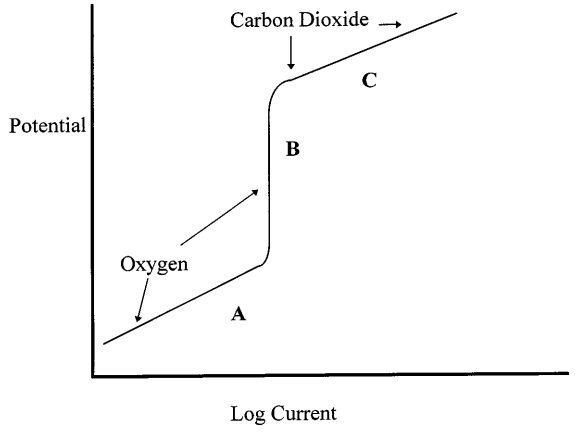

Fig. 9 Schematic log *i-E* relationship for a PA in alkaline electrolyte. *A* region of Tafel behaviour with oxygen evolution; *B* region of diffusion or reaction limited oxygen limited current; *C* region of Tafel behaviour with CO_2 evolution

Conclusions

The polyethylene-based material is unstable under anodic conditions in acid solutions where carbon dioxide is generated. In alkaline solutions, particularly those containing carbonate species, the stability is much greater because the anodic reaction is oxygen evolution. However, even in alkaline solutions there is some degradation of the carbon black because of the formation of humic acids.

Acknowledgements We would like to thank Raychem Ltd for their support of this work and EPSRC for the award of a studentship to B.J.E. and for assistance with the purchase of the FTIR equipment. We would also like to thank Prof. A. Hamnett for helpful discussions.

References

1. Bard AJ (1976) Encyclopedia of electrochemistry of the elements, vol 7. Decker, New York
2. Stonehart P (1984) Carbon 22: 423
3. Antonucci L, Romeo F, Minutoli M, Alderucci E, Giordano N (1987) Carbon 25: 197
4. Rositani F, Antonucci PL, Minutoli M, Giordano N. Villari A (1987) Carbon 25: 325
5. Giordano N, Antonucci PL, Passalacqua E, Pino L, Arico AS, Kinoshita K (1991) Electrochim Acta 36: 1931
6. Arico S, Antonucci V, Minutoli M, Giordano N (1989) Carbon 27: 337
7. Ross PN, Sokol H (1984) J Electrochem Soc131: 1742
8. Staud N, Ross PN (1986) J Electrochem Soc 133: 1079
9. Ross PN, Sattler M (1988) J Electrochem Soc 133: 1464
10. Staud N, Ross PN (1989) J Electrochem Soc 136: 3570
11. Fabish TJ, Schleifer DE (1984) Carbon 22: 19
12. Boehm HP (1994) Carbon 32: 759
13. Krishtalik LI, Rotenburg ZA (1966) Sov Electrochem 2: 322
14. Bardina G, Krishtalik LI, Rotenburg ZA (1966) Sov Electrochem 2: 199
15. Bardina G, Krishtalik LI (1966) Sov Electrochem 2: 306
16. Viet ND, Kokoulina DV, Krishtalik LI (1972) Sov Electrochem 8: 214
17. Viet ND, Kokoulina DV, Krishtalik LI (1972) Sov Electrochem 8: 218
18. Viet ND, Kokoulina DV, Krishtalik LI (1972) Sov Electrochem 8: 371
19. Viet ND, Kokoulina DV, Krishtalik LI (1972) Sov Electrochem 8: 374
20. Kokhanov GN, Milova NG (1969) Sov Electrochem 5: 82
21. Kokhanov GN, Milova NG (1970) Sov Electrochem 6: 64
22. Kokhanov GN (1971) Sov Electrochem 7: 1551
23. Beck F (1998) Graphite, carbonaceous materials and organic solids as active electrodes in metal-free batteries. In: Alkire RC (ed) Advances in electrochemical science and engineering, vol 5. Wiley-VCH, New York, p 335
24. Thiele H (1938) Trans Faraday Soc 34: 1033
25. Pierre C (1994) Anodeflex lifetime report. Raychem, Swindon, UK
26. Ives DJG, Janz JG (1961) Reference electrodes. Academic Press, New York
27. Weast RC (1992–3) Handbook of chemistry and physics, 73rd edn. CRC Press, Boca Raton, p 6–4
28. Christensen PA, Hamnett A, Hillman AR, Swann MJ, Higgins SJ (1992) J Chem Soc Faraday Trans 88: 595
29. Christensen PA, Hamnett A (1987) J Electroanal Chem 260: 347
30. Christensen PA, Hamnett A, Weeks SA (1988) J Electroanal Chem 280: 127
31. Balkast TI, Basturkt O, Gaines AF, Salihoglu I, Yilmaz A (1983) Fuel 62: 373
32. Socrates G (1994) Infrared characteristic group frequencies, 2nd edn. Wiley, New York
33. Compton RG, Hamnett A (1989) New techniques for the study of electrodes and their reactions. In: Compton RG (ed) Comprehensive chemical kinetics, vol 29, chap 1. Elsevier, New York
34. Yates JT Madey TE (1987) Vibrational spectroscopy of molecules on surfaces. Plenum Press, New York, p 6
35. Vesper SJ, Murdoch LC, Hayes S, Davis-Hoover WJ (1994) J Hazard Mater 36: 265